Chemistry and Physics of Lipids 221 (2019) 108–113

Contents lists available at ScienceDirect

Chemistry and Physics of Lipids

journal homepage: www.elsevier.com/locate/chemphyslip

Neutron diffraction of deuterated tripalmitin and the influence of shear on its crystallisation

B.H. Stuart[a,*], H.E. Maynard-Casely[b], N. Booth[b], A.E. Leung[c,1], P.S. Thomas[d]

[a] Centre for Forensic Science, University of Technology Sydney, 15 Broadway, NSW 2007, Australia
[b] Australian Centre for Neutron Scattering, Australian Nuclear Science and Technology Organisation, Locked Bag 2001, Kirrawee DC, NSW 2232, Australia
[c] National Deuteration Facility, Australian Nuclear Science and Technology Organisation, Locked Bag 2001, Kirrawee DC, NSW 2232, Australia
[d] School of Mathematical and Physical Sciences, University of Technology Sydney, 15 Broadway, NSW 2007, Australia

ARTICLE INFO

Keywords:
Tripalmitin
Neutron diffraction
Shear
Crystallisation

ABSTRACT

This neutron diffraction study of deuterated tripalmitin has provided further insight into a forensic observation of the crystallisation of lipids under high-shear conditions. To achieve this, an experimental set up was designed to enable simultaneous rheological data from a Couette cell to be recorded with neutron powder diffraction, enabling the influence of shear on the polymorph transformation on cooling to be monitored in real time. Tripalmitin was observed to directly transform from a liquid phase to a β polymorph under the influence of shear. Although the liquid to β transition was not observed to be influenced by shear rate, the degree of crystallinity, qualitatively denoted by an increase in the sharpness of the diffraction peaks, was observed at higher shear rates. Evidence is also presented that the rate of cooling influences the ordering in the β-polymorph produced in zero shear conditions.

1. Introduction

The appearance of unusual crystalline structures observed during a forensic post-mortem examination of a motor vehicle accident victim was the topic of an earlier study (Stuart et al., 2007). The crystal structures were found to be comprised of triacylglycerols (TAGs), the dominant lipid structure found in human adipose tissue, and the morphology of the crystalline material was proposed to be a result of shear stresses. However, the complexity of the TAG composition of adipose tissue made it difficult to elucidate the precise mechanism by which the crystalline structures were formed. In order to gain a better understanding of the influence of shear on adipose tissue, the shear behaviour of a model TAG, tripalmitin, has been investigated.

Tripalmitin is a monoacid TAG derived from palmitic acid. Tripalmitin is able to crystallise to three main polymorphs: α, β' and β. Each polymorph demonstrates specific hydrocarbon chain packing and thermal stability (Sato, 2001a, b; Lawler and Dimick, 2002). The α phase adopts hexagonal chain packing, while the β' phase exhibits orthorhombic packing. The most stable β polymorph forms triclinic chain packing. The formation of the various polymorphs depends upon the crystallisation conditions.

A number of studies have employed x-ray diffraction (XRD) methods to investigate the formation of polymorphism of tripalmitin (Sato and Kuroda, 1987; Kellens et al., 1990a, b; Hongisto et al., 1996). XRD is a popular tool for the study of TAG polymorphism as characteristic diffraction patterns can be identified for the different packing of each polymorph. Also, the influence of shear on the crystallisation of fats has been widely studied due to its industrial importance, particularly in the food industry. The application of shear is known to influence the nucleation and crystallisation processes of lipids (Mazzanti et al., 2005a; Tran and Rousseau, 2016). In order to understand shear induced effects in lipids, experiments involving the combination of XRD with a rheometer have been developed to provide a more direct examination of the nature of the crystallisation process under shear (Mazzanti et al., 2005a, 2003; Mazzanti et al., 2009, 2005b). These studies have demonstrated that a successful means of controlling shear has been with the use of a Couette cell, which consists of two concentric cylinders. The sample is placed between the cylinders and the inner cylinder is then rotated to generate the shear required.

The use of neutron diffraction for the study of TAG polymorphism has been limited due to the requirement of access to specialised instrumentation (Cebula et al., 1992). There is, however, a number of potential benefits to undertaking neutron diffraction measurements of tripalmitin. Neutrons scatter from the nucleus of each atom, an effective

* Corresponding author.
E-mail address: barbara.stuart-1@uts.edu.au (B.H. Stuart).
[1] Current address: Scientific Activities Division, European Spallation Source ERIC, Lund 224 84 Sweden.

https://doi.org/10.1016/j.chemphyslip.2019.02.011
Received 15 October 2018; Received in revised form 8 January 2019; Accepted 25 February 2019
Available online 29 March 2019

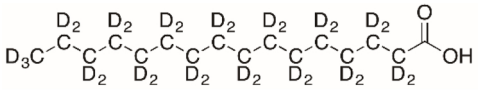

palmitic acid-d_{31}

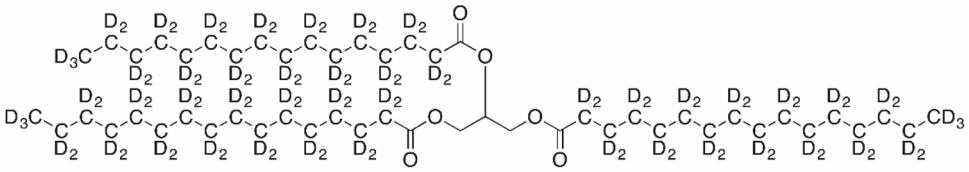

tripalmitin-d_{93}

Fig. 1. Structures of palmitic acid-d_{31} and tripalmitin-d_{93}.

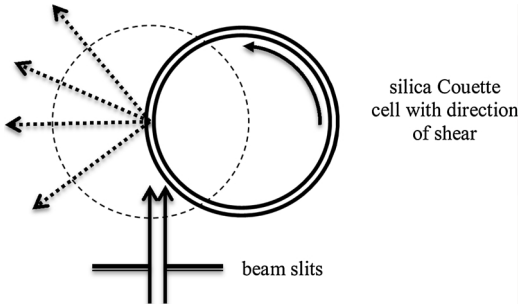

Fig. 2. Geometry of neutron instrument and shear cell. Solid arrows indicate the path of the incident neutron beam, and dashed arrows indicators of paths of the diffracted neutron beams. The dashed circle indicates the 50 mm diameter from the central sample position that is accepted by the radial collimator mounted before the detector.

point source, which means that neutron diffraction is not impeded by the form factor inherent in XRD and a wider angle of data to be more easily accessed. Additionally, compared to X-rays, neutrons are highly penetrating, which allows for *in situ* data to be collected from complex sample environments, such as shear cell environments. However, hydrogen (a large component in tripalmitin) is an incoherent scatterer of neutrons, which for experimental practicality leads to low signal-to-noise ratios of the measured diffraction. A common path to overcoming this limitation is to substitute deuterium into the structure, and as such, the deuterated tripalmitin structure has been investigated for this study.

In this study, neutron diffraction has been used to monitor the crystallisation processes of deuterated tripalmitin during cooling and in shear stress experiments controlled with a Couette cell. The tripalmitin was examined using a high intensity powder diffractometer in conjunction with a rheometer to shear the lipid sample while collecting diffraction data.

2. Materials and methods

2.1. Materials

Reagents were used as received from Sigma-Aldrich (USA). Solvents were used as received from Sigma-Aldrich or were purified by literature methods. The solvents for nuclear magnetic resonance (NMR) spectroscopy were used as received from Cambridge Isotope Laboratories Inc. (USA). Deuterium oxide (D_2O) (99.8%) was purchased from Atomic Energy of Canada Limited (Canada).

2.2. NMR spectroscopy

NMR spectroscopy was used to confirm the composition of the synthetic deuterated tripalmitin. ^{1}H NMR (400 MHz), ^{2}H NMR (61.4 MHz) and ^{13}C NMR (100 MHz) spectra were recorded using a Bruker 400 MHz spectrometer at 298 K. Chemical shifts were referenced to the residual signal of the solvent. ^{2}H NMR spectroscopy was performed using the probe's lock channel for direct observation.

2.3. Mass spectrometry

Mass spectrometry was used to determine the extent of deuteration in the tripalmitin synthesised. Electrospray ionisation mass spectra were recorded using a 4000 QTrap AB SCIEX mass spectrometer. The overall percentage deuteration of the molecules was calculated using enhanced resolution mass spectrometry (ER-MS). The isotope distribution of the different isotopologues was determined by analysing the area under each MS peak, which corresponds to a defined number of deuterium atoms. The contribution of the carbon13 (natural abundance) to the value of the area under each [X + 1] MS signal was subtracted based on the relative amount found in the unlabelled version (Duffin et al., 1991).

2.4. Synthesis of deuterated tripalmitin

Palmitic acid-d_{31} (Fig. 1) was first produced via metal-catalysed hydrothermal H/D exchange according to a method reported in the literature for azelaic acid-d_{14} and nonanoic acid-d_{17} (Darwish et al., 2013). ^{2}H NMR (61.4 MHz, $CDCl_3$) δ 0.83 (s), 1.20 (s), 1.59 (s), 2.31 (s). MS (ESI—) *m/z* calculated for $C_{16}D_{31}O_2$ $[M—H]^-$ as 286.4; found: 286.5 (100%). Deuteration: 97.9% by MS: isotope distribution: d_{27} 1.3%, d_{28} 2.9%, d_{29} 10.0%, d_{30} 30.4%, d_{31} 55.5%.

Palmitic acid-d_{31} (Fig. 1) (6.08 g, 21.1 mmol, 97.5% D by MS) and glycerol (588 mg, 6.38 mmol) were dissolved in dry dichloromethane (DCM) (75 mL). 4-Dimethylaminopyridine (DMAP) (826 mg, 6.76 mmol) was added. When all of the reagents had dissolved, the vessel was covered with foil and a 1.0 M solution of N,N'-dicyclohexylcarbodiimide (DCC) in DCM was added in aliquots: 10 mL (10 mmol)

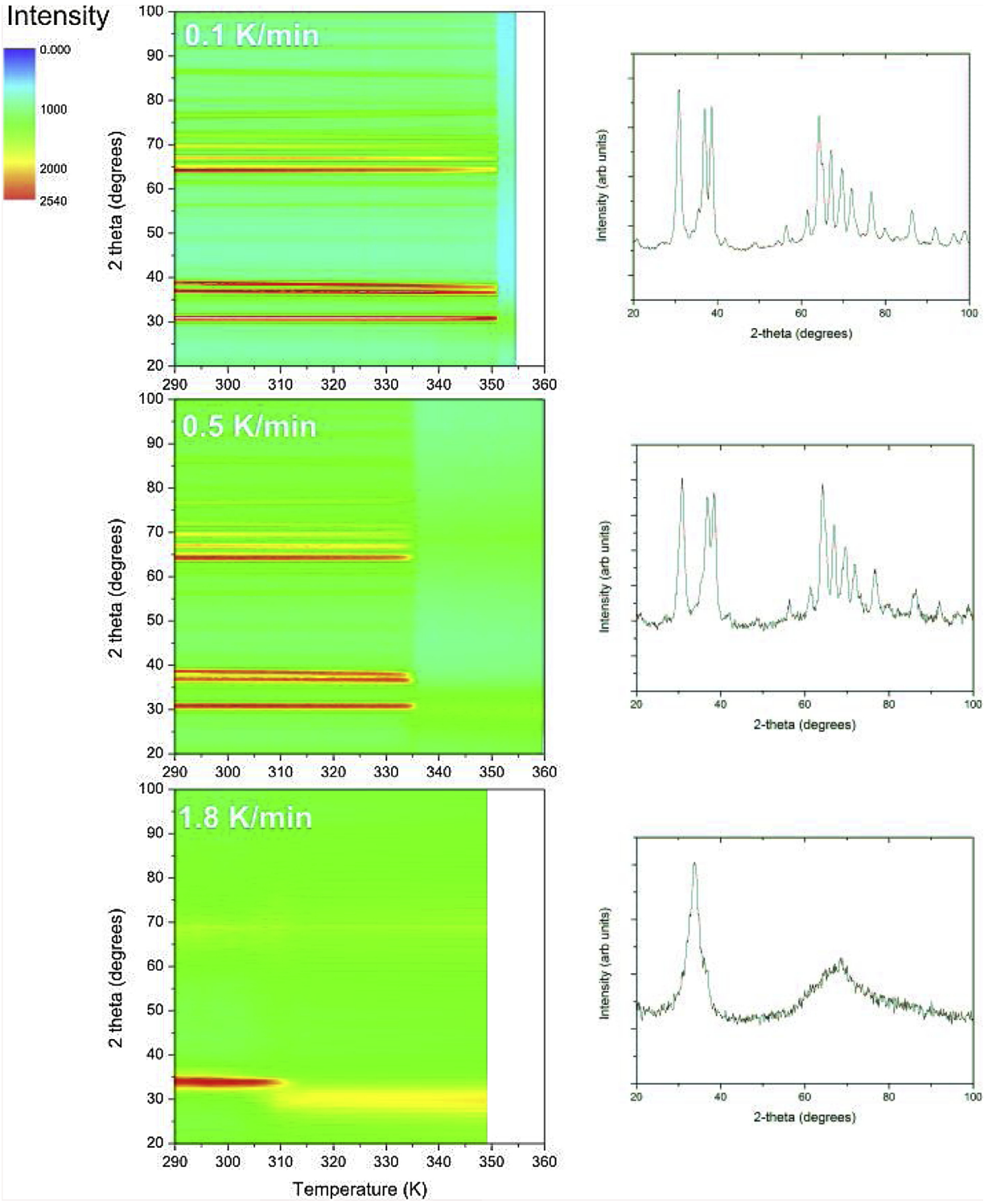

Fig. 3. Neutron diffraction data collected at a wavelength of 2.41 Å for different cooling rates within the cryofurnace (not from within the rheometer) and corresponding diffraction patterns collected at 300 K. Collection times for each pattern in the 0.1 K min^{-1} data was 5 min, for 0.5 K min^{-1} was 1 min and for the 1.8 K min^{-1} was also 1 min. Colours indicate the intensity of the diffraction pattern as per the scale bar.

initially; after 2 h another 5 mL (5 mmol); after an additional 18 h another 3.5 mL (3.5 mmol); after an additional 2 h another 3 mL (3 mmol) (total: 21.5 mL, 21.5 mmol). After 2 h, additional palmitic acid-d_{31} (562 mg, 1.85 mmol) and DCC (1.0 M in DCM, 5 mL, 5 mmol) were dissolved in dry DCM (10 mL) and added to the reaction mixture, which was allowed to stir at room temperature overnight. The mixture was filtered and concentrated under reduced pressure, then dissolved in 5% ethyl acetate (EtOAc) in petroleum ether and filtered again. The crude product was purified firstly by manual flash column chromatography (5% EtOAc in petroleum ether), then the fractions containing the product were combined, concentrated and the resulting solid recrystallised from EtOH to afford a white solid (1.88 g, 33%). ^{1}H NMR (400 MHz, $CDCl_3$) δ 0.82 (s, residual), 1.19–1.25 (complex, residual), 1.54 (s, residual), 2.27 (s, residual), 4.22 (AB quartet, J = 11.6, 6.0, 4.3 Hz, 4 H), 5.26 (m, 1 H). ^{2}H NMR (61.4 MHz, $CDCl_3$) δ 0.81 (s), 1.12 (s), 1.56 (s), 2.27 (s). ^{13}C NMR (100 MHz, $CDCl_3$) δ 13.1 (m), 21.5 (m), 23.9 (m),

Table 1
Diffraction parameters for deuterated tripalmitin polymorphs obtained using neutron diffraction.

2θ (°)	d-spacing (Å)	polymorph
30.8	4.54	β
33.6	4.17	α
36.9	3.81	β
41.5	3.40	β
64.1	2.27	β
68.4	2.14	α
69.5	2.11	β
76.5	1.95	β
80.4	1.87	β
91.6	1.68	β
99.3	1.58	β

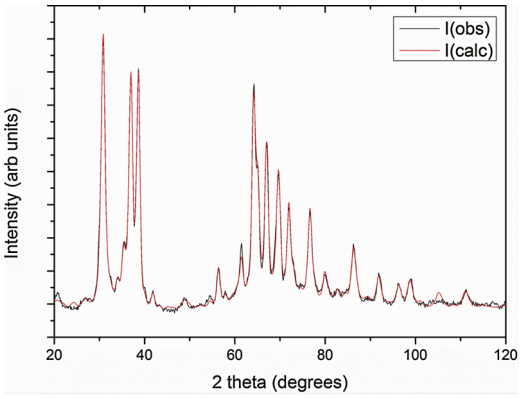

Fig. 4. Refinement of the neutron diffraction data collected at a wavelength of 2.41 Å during the 0.1 K min^{-1} cooling run at 300 K (I(obs)) versus the model of β phase of tripalmitin determined by Langevelde et al. (I(calc)) (van Langevelde et al., 1999). The variables of this model described in the text produced a fit RWP of 6.2% and GOF of 6.1%.

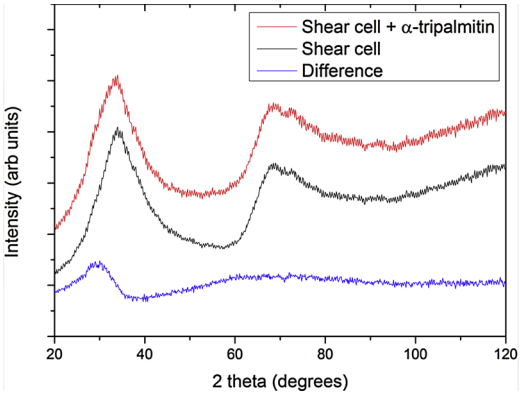

Fig. 5. Comparison of the diffraction patterns of the empty shear cell (black line) with that of the cell including α-tripalmitin (red line) collected at a wavelength of 2.41 Å and at 300 K. Data have been normalised to incident beam monitor counts. The blue line is the subtraction of the empty shear cell pattern from that including the α-tripalmitin, which at low angles shows the characteristic features of the α-tripalmitin diffraction pattern.

28.5 (m), 30.7 (m), 33.6 (m), 62.2 (s), 69.0 (s), 173.1 (s), 173.5 (s). MS (ESI+) *m/z* calculated for $C_{51}H_5D_{93}NaO_6$ $[M + Na]^+$ as 923.3; found: 922.5 (100%). Deuteration: 92.8% by MS: isotope distribution: d_{87} 0.7%, d_{88} 2.2%, d_{89} 5.7%, d_{90} 13.2%, d_{91} 24.7%, d_{92} 29.0%, d_{93} 24.5%.

2.5. Neutron diffraction

Neutron diffraction data was collected using the WOMBAT high intensity powder diffractometer at the Australian Centre for Neutron Scattering, Australian Nuclear Science and Technology Organisation (ANSTO) (Studer et al., 2006). The instrument was set up with a focusing germanium monochromator optimised to the [113] reflection so the wavelength of incoming neutrons was λ = 2.41 Å. Before the shear experiments were conducted, cooling experiments were undertaken within an orange cryostat mounted onto the WOMBAT instrument (Brochier, 1977) with the sample placed within a 70 mm length, 6 mm diameter vanadium can with thermocouples and heaters placed above and below the sample for temperature control. Three runs were conducted; two with the cooling controlled at 0.1 and 0.5 K min^{-1} and one 'rapid' cooling run where the heating was switched off, the rate of this cooling was determined to be 1.8 K min^{-1} on average. Collection times for each pattern during these cooling runs were 5 min, 1 min and 1 min, respectively. After these experiments were completed, the cryofurnace was removed and replaced with the rheometer. The deuterated tripalmitin specimens were then subjected to shear stress via the use of an Anton Paar MCR500 rheometer with an ANSTO designed silica Couette cell suitable for neutron scattering experiments. The layout of the cell within the instrument is illustrated in Fig. 2 (Booth et al., 2017), positioning of the apparatus was optimised with copper foil placed within the cell. The inner cylinder had a diameter of 48 mm and the gap between the inner and outer cylinders was 0.5 mm. The temperature was controlled by an external water jacket shaped so as not to obstruct the incoming neutron beam or the neutron detector. Two experimental runs were completed with this apparatus, both with the cooling rate controlled to 0.5 K min^{-1}, one with shear applied at 10 Hz and one with shear applied at 1000 Hz. For both of these experimental runs patterns were each 1 min.

2.6. Data analysis

Each diffraction pattern was collected on WOMBAT's continuous detector bank, located between 20-160° degrees around the sample position. The detector is 200 mm high and each collected pattern was integrated vertically to produce a one-dimensional plot. Each temperature's pattern was then stacked to produce thermodiffractograms presented in subsequent figures. Fitting of the diffraction data was undertaken using the TOPAS suite of programs (Coelho, 2008). Counting times of the diffraction data were varied during the course of the experiment and where data is compared in this publication, counts have been normalised to the incoming beam monitor before plotting.

3. Results and discussion

3.1. Neutron diffraction of deuterated tripalmitin

The formation of polymorphs by deuterated tripalmitin without shear was initially investigated by examining the structures formed under differing cooling rates within the cryofurnace set up. A cooling rate of 1.8 K min^{-1} from 350 to 280 K was employed to produce an α phase in the tripalmitin. A slower rate of 0.1 K min^{-1} from 360 to 290 K was used to produce a β phase. Fig. 3 shows the neutron diffraction data as a function of temperature collected for each of these rates, as well as the data for 0.5 K min^{-1}, the cooling rate chosen for the shear experiments. The corresponding diffraction patterns at a temperature of 300 K for each cooling rate are also shown in Fig. 3.

Table 1 lists the 2θ angles and the calculated d-spacing values for the peaks shown in the 300 K diffraction patterns produced at cooling rates of 0.1 and 1.8 K min^{-1} and may be attributed either the α or β phases. For the faster cooling rate of 1.8 K min^{-1}, a strong peak at 33.6° (4.17 Å) is indicative that the sample had formed into the α phase (Kellens et al., 1990a, b). The slower cooling rate of 0.1 K min^{-1} resulted in a number of diffraction peaks, notably at d-spacings of 4.54, 3.81 and 3.65 Å. Based on Kellen et al. reporting of three strong peaks in the XRD pattern at d-spacings of 4.60, 3.85 and 3.70 Å (Kellens et al.,

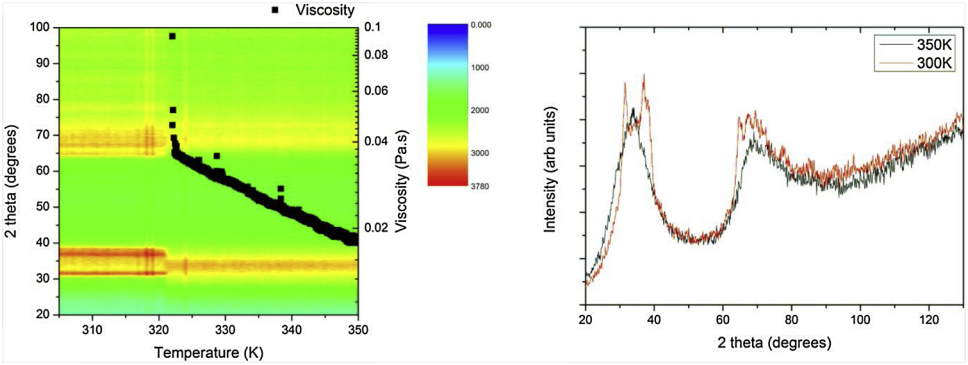

Fig. 6. Left hand image - diffraction data collected during cooling at 0.5 K min^{-1} and shearing at 10 s^{-1}. Colours indicate the intensity of the diffraction pattern (left axis) as per the scale and black squares chart measured viscosity (right axis). Right hand image - comparison between diffraction data collected at 350 and 300 K. Each pattern was collected for 1 min.

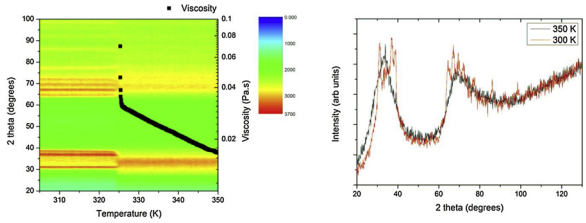

Fig. 7. Left hand image - diffraction data collected during cooling at 0.5 K min^{-1} and shearing at 1000 s^{-1}. Colours indicate the intensity of the diffraction pattern (left axis) as per the scale and black squares chart measured viscosity (right axis). Right hand image - comparison between diffraction data collected at 350 and 300 K. Each pattern was collected for 1 min.

1990b), it can be deduced that the sample had formed the β phase. The shift of ˜0.05 Å in the peak positions can be attributed to the differences in the sample positioning relative to the detectors between the XRD and neutron experiments. Table 1 also lists multiple peaks above 60° corresponding to d-spacings in the range 1.5–2.5 Å, that had not been noted by Kellen et al. These are higher angle peaks that are difficult to observe in XRD, such as the peak at 68.4° (2.14 Å), are resolved in the neutron diffraction data because of the lack of form factor.

The quality of the data is such that a refinement of the data was able to be undertaken against a model of the β tripalmitin crystal structure proposed by van Langevelde et al. (van Langevelde et al., 1999). This is presented in Fig. 4, and qualitatively shows a good fit to the triclinic $P\bar{1}$ unit cell with lattice parameters of $a = 5.42$ Å, $b = 11.98$ Å, $c = 40.31$ Å, $\alpha = 84.28°$, $\beta = 87.35°$ and $\gamma = 79.65°$, resulting in a volume of 2561 $Å^3$. Aside from the hydrogen atoms being replaced by deuterium atoms in the model, the refined parameters during the refinement in addition to the lattice parameters were scale factor, peak shape and an 8-term spherical harmonic preferred orientation model. This serves as excellent confirmation of the model determined by van Langevelde et al. from single crystal x-ray diffraction data.

The intermediate cooling rate used (0.5 K min^{-1}) also shows a β phase in the diffraction data collected at 300 K (Fig. 3). At 335 K, the pattern immediately changes to that of a β phase, indicating that this is the temperature at which the liquid → β transition occurs in the absence of shear. The 300 K diffraction pattern for the 0.5 K min^{-1} cooling rate shows slightly broader peaks than those observed in the pattern collected for the 0.1 K min^{-1} cooling rate, indicating differences in crystal size or perfection due to different cooling rates (Kellens et al., 1990b).

3.2. The influence of shear on the crystallisation of deuterated tripalmitin

Fig. 5 illustrates the background contribution of the shear cell, which is dominated by the silica from the cell and with some effects of air scattering at higher angles. The air scattering effects are removed when the cell is filled. This shows it is challenging to identify the presence of an α phase from within the cell other than in a possible broadening of the peak at ˜35°, which is revealed in more detail with the subtraction shown in Fig. 5.

Fig. 6 illustrates the diffraction data collected during cooling of the deuterated tripalmitin at a rate of 0.5 K min^{-1} and shearing at 10 s^{-1}. As the tripalmitin is cooled from 350 to 323 K, the viscosity values early in the experiment are low and correspond to a liquid phase. The patterns collected in this range show broad peaks near 35° and 68°. Although these peaks correspond to those predicted for the α-phase of tripalmitin, an inspection of the background contribution to the pattern by the shear cell reveals that these two peaks are from the cell itself.

As was observed in the diffraction data collected at zero shear, there is a clear transition to the β phase occurring as the tripalmitin cools under shear at 10 s^{-1} (Fig. 5). Although the background contribution of the shear cell is also overlapping with the β-phase peaks, the sharper contributions made by this polymorph is more readily discernible in the diffraction data shown in Fig. 5. The temperature at which the transition to the β phase appears to occur is lowered to 323 K compared to the 335 K liquid → β transition temperature observed in the cryofurnace measurements where no shear was applied. Viscosity measured during the experiment showed a gradual increase as the sample was cooled to 323 K, where the transition was observed in the diffraction data. The instigation of the transition also coincides with a very rapid increase in viscosity as cooling proceeds (Sonwai and Mackley, 2006; de Graef et al., 2008).

Similar findings to those observed at 10 s^{-1} were obtained for the data collected at a shear of 1000 s^{-1}. The diffraction data collected during cooling of the deuterated tripalmitin at a rate of 0.5 K min^{-1} and shearing at 1000 s^{-1} is shown in Fig. 7. A comparison of the peaks associated with the β phase observed in the diffraction data collected below 325 K for the 10 and 1000 s^{-1} shear rates indicates that sharper peaks are produced under 1000 s^{-1} (Figs. 5 and 7). The narrower peaks at the higher shear rate may be associated with a more ordered structure produced when higher shear forces are applied and are likely to be due to an increased degree of orientation of the TAG molecules at higher shear rates. Note that the instrument configuration used in this study is not set up to identify orientation effects.

The transition from a liquid phase to the β phase is observed to occur at 325 K at 1000 s^{-1}, again below that observed in the cryofurnace measurements with no shear, and solidification is also accompanied by a sharp increase in the viscosity. The increase in shear from 10 to 1000 s^{-1} appears to have no major influence on the crystallisation temperature of tripalmitin indicating that the reduction in the transition temperature is most likely to be due to differences in sample geometry rather than extraneous effects such as shear induced heating.

4. Conclusions

Neutron diffraction has been successfully applied to characterise the different polymorphic structures adopted by deuterated tripalmitin as it is cooled from the liquid state, and has confirmed previous single crystal determination of the triclinic β tripalmitin crystal structure.

Through the use of a shear cell in combination with the high intensity powder diffractometer it was possible to monitor the effect of shear stress on tripalmitin. A clear transition to a β-phase for this TAG was observed. The temperature at which the transition occurs is independent of shear rate used, but shear forces play a role in the degree of crystalline order when the β-polymorph is formed; a higher degree of order at higher shear rates indicates shear rate influences orientation. A limitation to the interpretation of any α-phase of tripalmitin was identified in this study due to the nature of the shear cell. However, there is scope to modify the materials employed and develop methods for the removal of the background contribution in further studies. This will enable the influence of shear to be further investigated for TAG systems of interest in a range of applications.

Conflict of interest

The authors declare no conflict of interest.

Acknowledgements

This work was supported by ANSTO's Australian Centre for Neutron Scattering Neutron Beam Instrument Access funding [grant number 3549] and National Deuteration Facility funding [grant number 3640].

References

Booth, N., Davidson, G., Imperia, P., Lee, S., Stuart, B.H., Thomas, P.S., Komatsu, K., Yamane, R., Prescott, S., Maynard-Casely, H.E., Nelson, A., Rule, K., 2017. Three impossible things before lunch - the task of a sample environment specialist. J. Neutron Res. 19, 49–56.

Brochier, D., 1977. Institut Laue-Langevin Technical Report 77/74.

Cebula, D.J., McClements, D.J., Povey, M.J.W., Smith, P.R., 1992. Neutron diffraction studies of liquid and crystalline trilaurin. J. Am. Oil Chem. Soc. 69, 130–136.

Coelho, A., 2008. TOPAS 4.1. Bruker AXS, Wisconsin, USA.

Darwish, T.A., Luks, E., Moraes, G., Yepuri, N.R., Holden, P.J., James, M., 2013. Synthesis of deuterated [D32] oleic acid and its phospholipid derivative [D64] dioleoyl-sn-glycero-3-phosphocholine. J. Label. Compd. Radiopharm. 56, 520–529.

de Graef, V., Goderis, B., Van Puyvelde, P., Foubert, I., Dewettinck, K., 2008. Development of a rheological method to characterise palm oil crystallising under shear. Eur. J. Lipid Sci. Technol. 110, 521–529.

Duffin, K.L., Henion, J.D., Shieh, J.J., 1991. Electrospray and tandem mass spectrometric characterisation of acylglycerol mixtures that are dissolved in nonpolar solvents. Anal. Chem. 63, 1781–1788.

Hongisto, V., Lehto, V.P., Laine, E., 1996. X-ray diffraction and microcalorimetry study of the α→β transformation of tripalmitin. Thermochim. Acta 276, 229–242.

Kellens, M., Meeussen, W., Reynaers, H., 1990a. Crystallisation and phase transition studies of tripalmitin. Chem. Phys. Lipids 55, 163–178.

Kellens, M., Meeussen, W., Riekel, C., Reynaers, H., 1990b. Time resolved X-ray diffraction studies of the polymorphic behaviour of tripalmitin using synchrotron radiation. Chem. Phys. Lipids 52, 79–98.

Lawler, P.J., Dimick, P.S., 2002. Crystallisation and polymorphism of fats. In: Akoh, C.C. (Ed.), Food Lipids: Chemistry, Nutrition and Biotechnology. Marcel Dekker, New York, pp. 275–300.

Mazzanti, G., Guthrie, S.E., Sirota, E.B., Marangoni, A.G., Idziak, S.H.J., 2003. Orientation and phase transitions of fat crystals under shear. Cryst. Growth Des. 3, 721–725.

Mazzanti, G., Marangoni, A.G., Guthrie, S.E., Idziak, S.H.J., Sirota, E.B., 2005a. Crystallisation of bulk fats under shear. In: Dutcher, J.R., Marangoni, A.G. (Eds.), Soft Materials – Structure and Dynamics. Marcel Dekker, New York, pp. 279–299.

Mazzanti, G., Marangoni, A.G., Idziak, S.H.J., 2005b. Modeling phase transitions during the crystallisation of a multicomponent fat under shear. Phys. Rev. E 71, 041607.

Mazzanti, G., Marangoni, A.G., Idziak, S.H.J., 2009. Synchrotron study on crystallisation kinetics of milk fat under shear flow. Food Res. Int. 42, 682–694.

Sato, K., 2001a. Crystallisation behaviour of fats and lipids – a review. Chem. Eng. Sci. 56, 2255–2265.

Sato, K., 2001b. Molecular aspects in fat polymorphism. In: Widlak, N., Hartel, R.W., Narine, S.S. (Eds.), Crystallisation and Solidification Properties of Lipids. AOCS Press, Champaign, pp. 1–15.

Sato, K., Kuroda, T., 1987. Kinetics of melt crystallisation and transformation of tripalmitin polymorphs. J. Amer. Oil Chem. Soc. 64, 124–127.

Sonwai, S., Mackley, M.R., 2006. The effect of shear on the crystallisation of cocoa butter. J. Amer. Oil Chem. Soc. 83, 583–596.

Stuart, B.H., Notter, S.J., Langlois, N., Maynard, P., Ray, A., Berkahn, M., 2007. Characterisation of the triacylglycerol crystal formation in adipose tissue during a vehicle collision. J. Forensic Sci. 52, 938–942.

Studer, A.J., Hagen, M.E., Noakes, T.J., 2006. Wombat: the high-intensity powder diffractometer at the OPAL reactor. Physica B 385-386, 1013–1015.

Tran, T., Rousseau, D., 2016. Influence of shear on fat crystallisation. Food Res. Int. 81, 157–162.

van Langevelde, A.J., van Malssen, K., Hollander, F., Peschar, R., Schenk, H., 1999. Structure of mono-acid even-numbered β-triacylglycerols. Acta Cryst. B55, 114–122.